Self-consistent optimization of neoclassical toroidal torque with anisotropic perturbed equilibrium in tokamaks

J.-K. Park[1], N. C. Logan[1], Z. R. Wang[1], J. E. Menard[1], A. H. Glasser[2], A. H. Boozer[3], E. Kolemen[4] and Y. In[5]

[1]Princeton Plasma Physics Laboratory, Princeton, New Jersey 08543, USA
[2]Fusion Theory and Computation, Inc., Washington 98346, USA
[3]Columbia University, New York, New York 10027, USA
[4]Princeton University, Princeton, New Jersey 08544, USA
[5]National Fusion Research Institute, Daejeon 34133, Korea

Corresponding Author: jpark@pppl.gov

Abstract:

A potentially promising actuator for rotation control in tokamaks is the non-axisymmetric (3D) magnetic perturbation, as it can substantially alter toroidal rotation by neoclassical toroidal viscosity (NTV). The optimization of the 3D field distribution for NTV and rotation control is however a highly complicated task, since NTV is mostly non-linear to the magnitude of the applied field with a complex dependency on the 3D field distribution. Here we present a new method that entirely redefines the NTV optimizing process, using the new general perturbed equilibrium code (GPEC). GPEC solves a non-self-adjoint force operator and force balance with the first-order change in pressure anisotropy by non-axisymmetry, and integrates its second-order change for NTV under the force balance. This self-consistent calculation uniquely yields the torque response matrix, enabling the NTV profile optimization by a single code run based on the full eigenmode structure of torque matrix. The code applications to non-axisymmetric control coil (NCC) design in NSTX-U showed the efficiency and accuracy of the new method, and in addition the importance of the backward helicity modes and self-shielding by torque in NTV control. The access to the optimized field distribution is limited in practice, but it is also straightforward to couple a given set of coils to torque matrix and optimize the current distributions in the coils.

1 Introduction

An important utility of non-axisymmetric (3D) magnetic perturbation in tokamaks can be found in the control of toroidal rotation, since 3D magnetic perturbation can generate non-ambipolar neoclassical process and thus alter $\vec{E} \times \vec{B}$. This process can be understood by the injection of torque, due to neoclassical toroidal viscosity (NTV) when axisymmetry is broken. The variability of NTV torque and its profile across radius is in principle as

large as the shape of 3D magnetic perturbations, which makes NTV potentially promising for torque control. The optimization of 3D field or coils for NTV, however, is a highly complicated task due to two main reasons; (1) NTV is a transport non-linear to the 3D field spectrum, and (2) the 3D field spectrum is established with plasma response in equilibrium. This means that one should couple the models for 3D plasma equilibrium and transport, and examine the coupled non-linear outcomes to address the variability of NTV torque by 3D field. The optimization of coils, or assessment of coil capabilities to drive local NTV, was extensively explored in the course of non-axisymmetric control coil (NCC) design and physics studies for NSTX-U. An important application of stellarator optimizer was made during the studies, by coupling IPEC-PENT to STELLOPT, called IPECOPT, as published in [1]. However, this method still required typically about $10^2 \sim 10^3$ code runs to find the best 3D field to generate the target NTV profile form assigned, and also left the issue whether the iteratively estalished solution is merely a local extrenum or truly a global optimum. This motivated the development of a new method using general perturbed equilibrium code (GPEC), which entirely redefines the NTV optimizing process through the self-consistent torque response matrix, which will be described in this report.

This proceeding is organized as follows, after this Introduction. Section 2 will give the essence of theoretical formulations and results, and show briefly how to derive torque response matrix. Section 3 will discuss briefly the feature of GPEC solutions as well as numerical benchmark with MARS-K. The torque response matrix then will be used to illustrate how to optimize NTV torque profile in free space and also with a given set of coils in Section 4, and then the proceeding will be concluded with remarks.

2 GPEC formulation and Torque Response Matrix

The force balance equation including anisotropic pressure tensor driven by non-axisymmetric field is given by

$$\delta\vec{F} = \delta\vec{j} \times \vec{B} + \vec{j} \times \delta\vec{B} - \vec{\nabla}\delta p - \vec{\nabla} \cdot \left((\delta p_\parallel - \delta p_\perp)\hat{b}\hat{b} + \delta p_\perp \overleftrightarrow{I} \right) - \delta\vec{F}_g = 0, \qquad (1)$$

with two Maxwell relations $\delta\vec{j} = \vec{\nabla} \times \delta\vec{B}$ and $\delta\vec{B} = \vec{\nabla} \times (\vec{\xi} \times \vec{B})$. The adiabtic part of perturbed pressure arising by Lagrangian formulation is given by $\delta p = -\vec{\xi} \cdot \vec{\nabla} p$. The general perturbed equilibrium code (GPEC) is formulated to include "general" non-axisymmetric force $\delta\vec{F}_g$, which will be omitted here to focus on the self-consistent NTV calculations. In the first gyro-radius ordering, the perturbed anisotropic pressures $\delta p_\parallel = \int d^3v M v_\parallel^2 \delta f$ and $\delta p_\perp = \int d^3v (M v_\perp^2/2) \delta f$ become

$$\delta p_\parallel = \sum_{s\sigma} \frac{2\pi B}{M_s^2} \int dE \int d\mu \frac{2(E - \mu B)}{|v_\parallel|} \delta f_{s\sigma}, \quad \delta p_\perp = \sum_{s\sigma} \frac{2\pi B}{M_s^2} \int dE \int d\mu \frac{\mu B}{|v_\parallel|} \delta f_{s\sigma}. \quad (2)$$

Here s stands for species and $\sigma \equiv sign(v_\parallel)$ representing co and counter rotating particles. The perturbed distribution function is neoclassically determined by drift-kinetic equation, and can differ if approximations or different collisional models are adopted. In any case,

one can see that collisions introduce the imaginary term in $\delta W = -(1/2)\int \vec{\xi}\cdot\delta\vec{F}$ as well as breaking the self-adjointness. Therefore, the standard variational method for δW cannot be used, and the force balance equation must be solved directly for each component.

The parallel balance implies just $\vec{\nabla}\cdot\left((\delta p_\parallel - \delta p_\perp)\hat{b}\hat{b} + \delta p_\perp \overleftrightarrow{I}\right) = 0$, which then gives a simple constraint $\hat{b}\cdot\vec{\nabla}\delta f = 0$, that is, the perturbed distribution function must be constant along the field lines as $\delta f = \delta f(E,\mu,\psi,\alpha)$. This leads to the orbit- averaged drift kinetic formuation under the action variation. Using the Hastie-Taylor form [2],

$$\frac{\partial \delta f}{\partial t} - \frac{1}{q\chi'}\left(\frac{\mathcal{J}_\psi}{\mathcal{J}_U}\frac{\partial \delta f}{\partial \alpha} - \frac{\delta \mathcal{J}_\alpha}{\mathcal{J}_U}\frac{\partial f_M}{\partial \psi}\right) - \frac{\delta \mathcal{J}_t}{\mathcal{J}_U}\frac{\partial f_M}{\partial U} = \hat{C}_b[\delta f], \tag{3}$$

where $\mathcal{J} \equiv \oint M v_\parallel dl$, $\chi' = d\psi_p/d\psi$, the guiding center energy $U \equiv E + q\phi$, and the subscript for $\mathcal{J}$ denotes the partial derivatives. Various authors used different assumptions to solve this equation. GPEC formulation can include the traditional Kruskal-Obermann [3] or CGL in the collisionless limit, as well as $1/\nu$ or ν regime formulation [4] or combined NTV formulation [5] for example.

The paralle force balance also eliminates $\xi_\parallel$, and the two remaining components of $\vec{\xi}$ can be determined by toroidal (or poloidal) and radial force balance. With Fourier representation for $\xi = \sum_{mn}\xi_{mn}e^{i(m\theta - n\varphi)}$, one can derive non-Hermitian Euler-Lagrange equation

$$(\mathbf{F}\Xi'_\psi + \mathbf{K}_R\Xi_\psi)' - (\mathbf{K}_L^\dagger\Xi'_\psi + \mathbf{G}\Xi_\psi) = 0, \tag{4}$$

where Ξ_ψ is the matrix vector and its elements are the Fourier modes of radial displacement $\vec{\xi}\cdot\vec{\nabla}\psi$, and $\mathbf{F}$, $\mathbf{K}_R$, $\mathbf{K}_L$, $\mathbf{G}$ are non-Hermitian $M\times M$ matrices with M number of Fourier modes containing drift-kinetic effects. More details for the matrices and formulation will be given in [6]. As shown in [7], it becomes toroidal Glasser equation in the ideal limit with $\mathbf{F}_I = \mathbf{F}_I^\dagger$, $\mathbf{K}_I = \mathbf{K}_{LI} = \mathbf{K}_{RI}$, $\mathbf{G}_I = \mathbf{G}_I^\dagger$. The equation (4) includes the force by anisotropic pressure tensor in the first order, and the force by anisotropic pressure tensor in the second order is precisely what is called NTV torque.

The second order energy and torque can be obtained by integrating $\int\vec{\xi}\cdot\delta\vec{F}$, finally giving

$$2\delta W + i\frac{\tau_\varphi}{n} = \int d\psi\left[\Xi_\psi^\dagger\left(\mathbf{F}\Xi'_\psi + \mathbf{K}_R\Xi_\psi\right)\right]' - \left[\Xi_\psi^\dagger\left((\mathbf{F}\Xi'_\psi + \mathbf{K}_R\Xi_\psi)' - (\mathbf{K}_L^\dagger\Xi'_\psi + \mathbf{G}\Xi_\psi)\right)\right] \tag{5}$$

$$= \left[\Xi_\psi^\dagger\left(\mathbf{F}\Xi'_\psi + \mathbf{K}_R\Xi_\psi\right)\right] = \Xi_\psi^\dagger\mathbf{W}_P\Xi_\psi. \tag{6}$$

due to the force balance by Euler-Lagrange equation. Here $\mathbf{W}_P$ can be called plasma response matrix, representing energy and torque driven by Ξ_ψ, and its anti-Hermitian part of $\mathbf{W}_P$ gives the torque response matrix. Changing the basis from Ξ_ψ to the external field on the boundary Φ, or to the current distributions C in a set of coils, one can construct

$$\tau_\varphi(\psi) = \Phi^\dagger\mathbf{T}(\psi)\Phi = C^\dagger\mathbf{T}_C(\psi)C \tag{7}$$

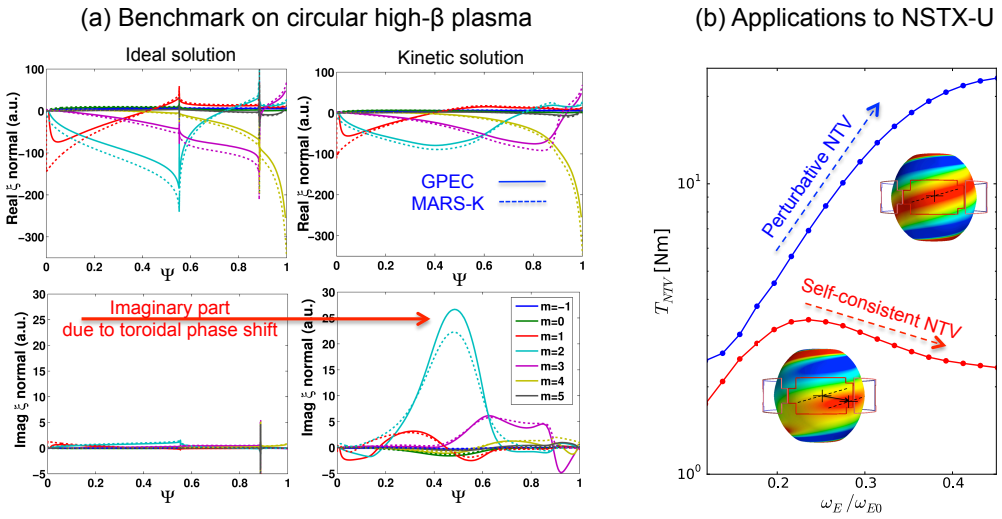

FIG. 1: (a) Comparison of GPEC and MARS-K solutions in both ideal and kinetic zero-frequency limit, and (b) GPEC applications to NSTX-U illustrating NTV self-shielding effects.

where $\mathbf{T}_{(C)} = \mathbf{T}^{\dagger}_{(C)}$ itself. With $\mathbf{T}$ one can calculate the (NTV) torque right away by calculating "external" (meaning "vacuum") 3D field on the plasma boundary Φ and make the quadratic operation as given. One can further change the basis from the external field to a vector representing the currents in the coils. If a row of coil can be represented by a complex number, that is, by its amplitude and toroidal phase for a fixed n, the k number of rows will constitute a complex vector matrix with a length k. By lineary mapping C to Φ, one can also construct a "coil-constrained" torque response matrix as shown in the equation. C can only create a subset of Φ, and $\mathbf{T}_C$ with a reduced dimension to $k \times k$ represents torque density profile that can be generated by a given set of coils.

3 Numerical Implementation and Benchmark

This section will briefly discuss the code implementation and benchmark. GPEC integrates the new Euler-Lagrange equation using LSODE package and thus on the adaptive radial grid, and couples the solutions to the external field and coils based on virtual casing method. This is similar to DCON and IPEC, but non-Hermitian Euler-Lagrange equation does not have any singularity as $det|\mathbf{F}| \neq 0$ in general, due to the anti-Hermitian part of the matrix.

The solution structure by GPEC should be in principle identical to the one by MARS-K code in zero-frequency limit, and if the same kinetic model is adopted. Numerical benchmark between these two self-consistent kinetic calculations was shown in Fig. 1 (a), on a circulr cross-section plasma but with low aspect ratio $A = 2.8$ and high $\beta_N = 3.3$ to magnify mode coupling effects as well as kinetic effects. In addition to the good agreement

made, one can see that there are new structure arising in imaginary part by both codes. In this example, the applied field is real (cosine) and plasma response is expected to be real if the force operator is Hermitian. This is why a circular plasma is selected. The coupling to imaginary (sine) is the consequence of torque, represented by this toroidal phase-shift in plasma response.

Another aspect one can see from Fig. 1 (a) is that the singular nature in the ideal solutions (left) across rational surfaces is disappeared in kinetic solutions. The singular behavior in the ideal solutions is integrable for ideal energy δW_I, but not for kinetic energy and torque. This is because transport depends on $\delta B_L = \delta B + \vec{\xi}\cdot\vec{\nabla}B$, inherently on a Lagrangian frame, and the tangential displacement $\xi_\alpha \propto \xi_\psi/(\psi-\psi_R)$ when $\psi \to \psi_R$ gives non-integrable singularity in δB_L. Therefore in the perturbative kinetic or NTV calculations, this singularity from plasma response should be regularized as reported in various literature [8-9].

The inclusion of torque in equilibrium can alter response and NTV calculations not only in the neighborhood of resonant surfaces, but also globally in a significant amount. Fig. 1(b) shows that perturbative vs. self-consistent NTV calculations for a high-β ($\beta_N = 3.4$) $I_P = 2.0MA$ NSTX-U plasma . The model equilibrium and kinetic profiles were simulated with TRANSP with 12MW NBI, but then ω_E is scaled from the given ω_{E0} to predict NTV dependency on rotation. In this particular example, the predicted NTV torque increases unrealistically more than $10Nm$ along with ω_E, but such a large torque creates currents and toroidal phase-shift that can shield external perturbation and eventually decrease NTV. This so-called self-shielding process was predicted by Boozer [10], and here demonstrated by numerical calculations for the first time.

4 Systematic optimization of NTV torque

The torque matrix functions derived in Sec. 2 can immediately answer some fundamental questions in NTV optimization; Let $\lambda[\mathbf{A}]$ be eigenvalues of the matrix $\mathbf{A}$.

- *Maximum (minimum) NTV torque achievable inside a given ψ, and how to create such a torque ideally or with a given set of coils?*:
  $\to \lambda_{\max(\min)}[\mathbf{T}(\psi)]$ without constraints and $\lambda_{\max(\min)}[\mathbf{T}_C(\psi)]$ when coil-constrained, with each proper normalization, e. g. $|\Phi| = 1G$ or $|C| = 1kA$. Each eigenvector gives the field required on the boundary or coil amplitude/phase needed.

- *Maximum (minimum) fraction of NTV torque achievable inside a given ψ, and how to achieve it ideally or with a given set of coils?*:
  $\to \lambda_{\max(\min)}\left[\mathbf{T}(\psi)\mathbf{T}^{-1}(\psi_b)\right]$ without constraints and $\lambda_{\max(\min)}\left[\mathbf{T}_C(\psi)\mathbf{T}_C^{-1}(\psi_b)\right]$ when coil-constrained, where $\psi_b = 1$ at the boundary. Each eigenvector gives the field required on the boundary or coil amplitude/phase needed.

- *Optimized NTV torque profile maximizing torque inside (ψ_1, ψ_2) while minimizing torque elsewhere when the total torque is fixed, and how to create such a torque ideally or with a given set of coils?*:

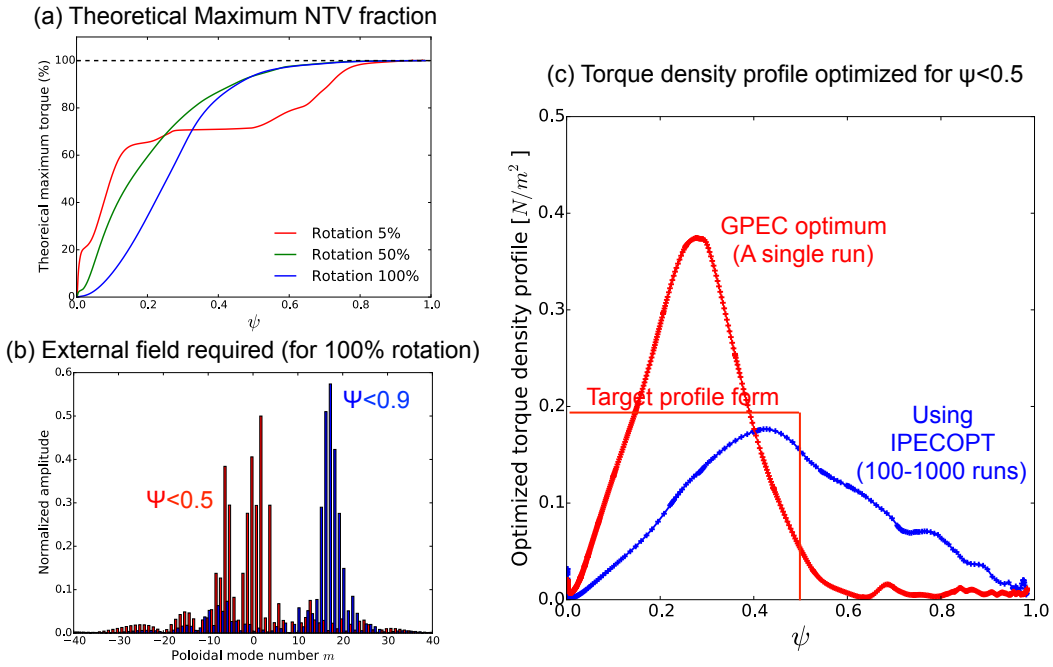

FIG. 2: (a) Maximum NTV torque fraction achievable ideally inside a given ψ for an NSTX-U model, (b) required field spectrum on the boundary to achieve them, and (c) resulting torque profile (for $\psi < 0.5$) and comparison with IPECOPT solution.

$\rightarrow \lambda_{\max(\min)} \left[\left(\mathbf{T}(\psi_2) - \mathbf{T}(\psi_2) \right) \mathbf{T}^{-1}(\psi_b) \right]$ and $\lambda_{\max(\min)} \left[\left(\mathbf{T}_C(\psi_2) - \mathbf{T}_C(\psi_2) \right) \mathbf{T}_C^{-1}(\psi_b) \right]$ with and without constraints by coils, respectively. Each eigenvector gives the field required on the boundary or coil amplitude/phase needed.

Here one ansatz required to use $\mathbf{T}^{-1}$ is the positive definitness in $\mathbf{T}$. If $\mathbf{T}$ is not a positive definite matrix, the second and third questions are ill-posed. The maximum torque fraction achievable at a given radius is shown in Fig. 2 (a) for an example, using NSTX-U target used for Fig. 1 (b). This is theoretical for the given target and kinetic profiles if any external field can be generated. It is surprising to see that one can dump 90% torque inside $\psi < 0.5$ depending on the kinetic profiles. Fig. 2(b) shows external field required to maximize NTV torque fraction for $\psi < 0.5$ and $\psi < 0.9$, indicating the importance of negative helicity (or minus m) modes to maximize torque in the core. This example of NTV optimization for core (here $\psi < 0.5$) was in fact extensively studied with IPECOPT method previously, which couples the perturbative NTV calculations by IPEC and PENT to STELLOPT. The iteratively obtained profile, as shown in Fig. 2(c), was one of major accomplishments in IPECOPT applications but GPEC can answer the same question immedicately by eigenvalue and eigenvector analysis. Besides, the optimized profile, shown also in Fig 2. (c), meets the requirements much better, indeed minimizing the NTV torque density outside $\psi = 0.5$. At this point it is not clear if this difference is due to self-consistent NTV vs. perturbative NTV, or global optimum by GPEC vs. local optimum by IPECOPT.

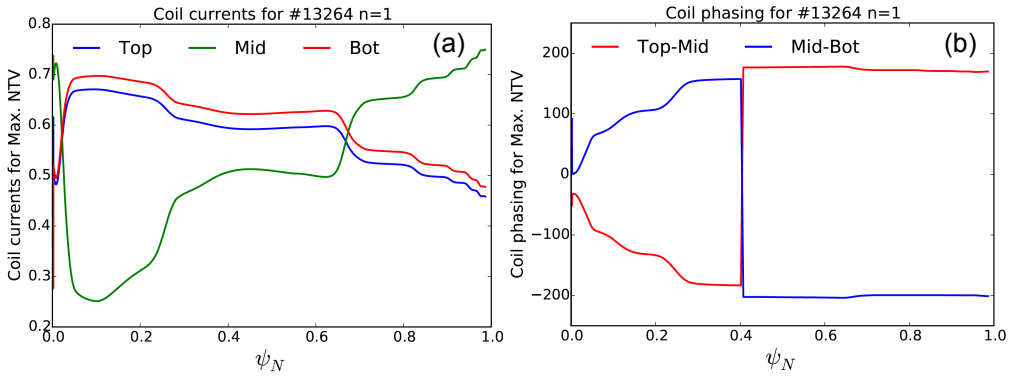

FIG. 3: (a) Coil currents and (b) phase-shifts required for each row for a KSTAR target (discharge #13264) to maximize NTV torque inside a given ψ.

Theoretical optimization illustrated above can be used to understand fundamental field coupling to NTV, and can suggest how one should shape the external field and design the coils accordingly. When a set of coils is given, however, one would want to answer the same questions with only field spectrum accessible by coils. This coil-constrained optimization is under investigations for new non-axisymmetric control coil (NCC) design for NSTX-U, and with I+C-coil in DIII-D, and also with IVCC coil system in KSTAR, and eventually can be used to optimize NTV with ITER RMP or EFC coils. Here for example, KSTAR has 3 rows of coils with 4 toroidal arrays, and thus $n = 1$ field can have arbitrary amplitude (up to $5kA$, which is the value supported by present power supplies) and toroidal phase from each row. This constitutes 3×1 complex vector C, representing amplitude and phase for each row in each element, and 3×3 coil-constrained torque response matrix $\mathbf{T}_C$ for KSTAR. The optimization of the coil current amplitudes and phases to maximize NTV torque inside a given ψ is shown in Fig. 3. (a) shows currents required with a normalization $I^2_{TOP} + I^2_{MID} + I^2_{BOT} = 1$, and (b) shows how to shift toroidal phase among coils. One toroidal phase is just a reference toroidal phase that does not change NTV unless intrinsic error field is significant. If only total NTV torque is concerned, one can easily see from the rightmost point that $I_{MID} \sim 2I_{TOP} \sim 2I_{BOT}$ and phase-shift (phasing) $160^o \sim 170^o$ can maximize total NTV torque. The eigenvalue indicates then that maximum total torque possible in this KSTAR target (#13264 from experiments) is $\sim 2Nm$ if *rms* current for coils allowed is up to $5kA$.

5 Concluding Remarks

The newly developed GPEC directly solves a non-self-adjoint force including kinetic anisotropic pressure tensor, to the first order of non-axisymmetric perturbation, and gives the second-order energy and torque. The solutions are self-consistent across equilibrium and neoclassical transport, giving more precise NTV calculations without adhoc assumption across resonant surfaces. One of unique features in GPEC is the torque response

matrix, which contains all the information of NTV torque that can be generated in free space or with a given set of coils, and thus NTV optimization can be greatly simplified by its eigenvalues and eigenvectors. Much more complicated questions, such a maximizing torque in (ψ_1, ψ_2) but minimizing torque (ψ_3, ψ_4) when the total torque is fixed, and/or when $|\Phi|$ or $|C|$ is fixed, can also be easily studied and answered using quadratic matrix optimizers rather than dealing with full non-linearly coupled plasma response and transport calculations. This work was supported by DOE Contract No. DE-AC02-09CH11466.

References

[1] LAZERSON, S. A., PARK, J.-K., et al., "Numerical optimization of three-dimensional coils for NSTX-U", Plasma Phys. Control. Fusion 57 (2015) 104001.

[2] HASTIE, R. J., TAYLOR, J. B., et al., "Adiabatic invariants and the equilibrium of magnetically trapped particles", Ann. Phys. 41 (1967) 302.

[3] KRUSKAL, M. D., OBERMAN, C. R., et al., "On the stability of plasma in static equilibrium", Phys. Fluids 1 (1958) 275.

[4] SHAING, K. C., "Magnetohydrodynamic-activity-induced toroidal momentum dissipation in collisionless regimes in tokamaks", Phys. Plasmas 10 (2003) 1443.

[5] PARK, J.-K., BOOZER, A. H., et al., "Nonambipolar transport by trapped particles in tokamaks", Phys. Rev. Lett. 102 (2009) 065002.

[6] PARK, J.-K., LOGAN, N. C., et al., "Perturbed equilibria in tokamaks consistent with neoclassical toroidal torque" (To be submitted).

[7] GLASSER, A. H., "The direct criterion of Newcomb for the ideal MHD instability of an axisymmetric toroidal plasma", Phys. Plasmas 23 (2016) 072505.

[8] BERKERY, J. W., LIU, Y. Q., "Benchmarking kinetic calculations of resistive wall mode stability", Phys. Plasmas 21 (2014) 052505.

[9] SUN, Y., LIANG Y., "Non-resonant magnetic braking on JET and TEXTOR", Nucl. Fusion 52 (2012) 083007.

[10] BOOZER, A. H., "Error field amplification and rotation damping in tokamak plasmas", Phys. Rev. Lett. 86 (2001) 5059.